JOURNAL OF THEORETICAL AND APPLIED MECHANICS
44, 3, pp. 585-602, Warsaw 2006

STATISTICAL DAMAGE MECHANICS – CONSTITUTIVE RELATIONS

Antonio Rinaldi
Dusan Krajcinovic

Mechanical and Aerospace Engineering, Arizona State University, Tempe, USA
e-mail: antnio.rinaldi@gmail.com

Sreten Mastilovic

Center for Multidisciplinary Studies, University of Belgrade, Belgrade, Serbia and Montenegro
e-mail: misko3210@yahoo.com

The statistical damage model presented by the authors in the previous paper of this series is used to formulate analytical constitutive relations for the hardening and softening phases of two-dimensional lattices. A proper definition of the damage parameter for the softening is introduced. The results confirm that the analytical model can be used for the study of the softening phase and failure. This research offers a seminal basis for Damage Tolerance Principles technology standards of the commercial airplane industry.

Key words: failure, statistical damage mechanics, damage tolerance, damage parameter, constitutive relations, scaling

1. Introduction: damage tolerance principles

A material microstructure containing many randomly distributed microcracks is initially statistically homogeneous, but becomes heterogeneous due to propagation of microcracks and their clustering into a macrocrack close to failure. Krajcinovic and Rinaldi (2005a) discuss the homogeneous-to-heterogeneous phase transition using the analytical tools of statistical mechanics, thermodynamics and fractal geometry. The threshold of failure depends on the structural transformations of the material on the microscale and the structure size. The limit states design is driven by crack growth, but also by the structural rearrangements in the material microstructure in the heterogeneous phase. The

base of structural design and maintenance principles in Boeing Commercial Airplane Group, U.S.A., is the "Damage Tolerance Principles" (Goranson, 1993), which is focused on two structural design objectives:

1. Damage Tolerance: ability of structure to sustain anticipated loads in the presence of fatigue, corrosion or accidental damage until such damage is detected through inspections or malfunctions and repaired;
2. Durability: ability of the structure to sustain degradation from such sources as fatigue, accidental damage and environmental deterioration to the extent that they can be controlled by economically acceptable maintenance and inspection programs.

Damage tolerance comprises three elements of importance for achieving the desired level of safety. The first element is the determination of the residual strength or the maximum allowable damage (including multiple secondary cracks) that the structure can sustain under regulatory fail-safe load conditions. The second element is the crack growth defined as the interval of damage progression from lengths with negligible probability of failure to an allowable size determined by the residual strength. Finally, a damage detection strategy (Inspection Program) must be adopted. The sequence of inspections in a fleet of airplanes requires methods and intervals selected to achieve timely the damage detection.

Fig. 1, adopted from Goranson (1993), shows typical experimental data from both full-scale crack growth testing (600 tests on two different wing-panels of width 200 mm and 2300 mm) and Linear Elastic Fracture Mechanics (LEFM). The crack length is normalized to the LEFM limit L_y and the strengths are normalized to the maximum strength of pristine undamaged panel. The maximum allowable damage (i.e. the minimum normalized strength) and the corresponding maximum defect length are assigned on such a graph in compliance with a "fail-safe" strategy. Nevertheless, the choice of the tolerable damage is largely based upon experience and the Probability Of Detection (POD) from visual inspections. Full-scale tests are necessary to assess the effect of the structural size on the damage tolerance, but Goranson recognizes the "impossibility" of conducting full-size fracture and fatigue tests to obtain the data in Fig. 1 for all the components. "The emphasis on residual strength verification has gradually shifted in recent years from wing structures to fuselage pressure shells" because "the extended use of jet transport structures raised concerns about multiple site damage in fuselage structures" (Goranson, 1993), which lead to expensive full-scale tests (of the order of millions of dollars) with large pressure test fixtures. Unfortunately, LEFM is not always applied to multiple-site cracking and diffuse damage, which is nowadays

still managed in a purely empirical manner. In conclusion, there is an urge to formulate more reliable multiscale analytical models that account for the structural size effect and which can be used for data extrapolation. The capability of estimating the POD a priori from such models would likely have a deep impact on the fail-safe strategy.

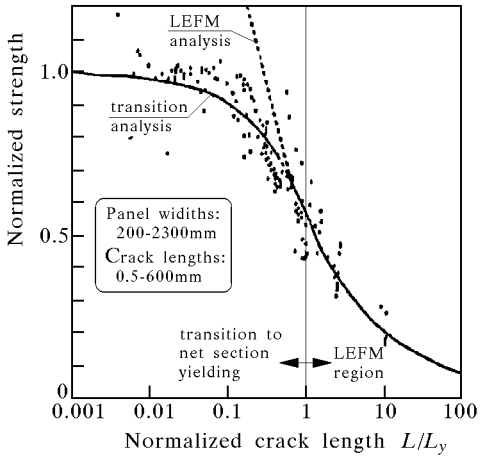

Fig. 1. Sample data of crack growth experiments on wing panels used at Boeing Co. (Goranson, 1993); L_y – boundary between LEFM and transition behavior

Goranson's "Damage Tolerance Principles" expresses the concern about the "lack of interest" in the scientific community to characterize and quantify the POD. This paper shows how the ideas discussed in the first part of this series (Krajcinovic and Rinaldi, 2005a), although in their infancy stage, could potentially address this concern and the other needs of damage tolerant design. The time-independent damage model (Kachanov, 1958) $\overline{\sigma} = \overline{E}^o(1 - \overline{D})\overline{\varepsilon}$, relating the macrostress $\overline{\sigma}$ and the macrostrain $\overline{\varepsilon}$, is obtained for the uniaxial tensile response of two-dimensional disordered spring networks through the damage parameter $\overline{D}$ and the corresponding scaling relations in Krajcinovic and Rinaldi (2005a). $\overline{E}^o$ is the elastic modulus of pristine state and the bar above the symbols indicates a macroscale quantity.

2. Lattice simulations and numerical data

The goal of this paper is to elucidate the universal behavior of the damage parameters and to infer constitutive relations of the quasi-brittle materials. The

disordered discrete model used for that purpose, although admittedly simple, captures what we believe to be the key features of the problem at hand. The approach taken in this paper is following footsteps of the extensive work on the central-force lattices modeling the brittle fracture of disordered materials (for example, Curtin and Scher, 1990; Hansen *et al.*, 1989, Krajcinovic and Basista, 1991). The model does not aim at describing a specific material but rather a class of quasi-brittle materials, whose primary microstructural failure mode is rupture of interfaces of inferior strength (compared to that of the bulk). Examples include the monolithic polycrystalline ceramics with inferior grain-boundary strength, ceramic composites with inferior particle-matrix interface strength, polyphase materials with weak phase interfaces, as well as concrete, clastic rocks, etc. The common feature of these materials, which is essential for adequacy of the proposed microstructural modeling, is that the interfacial (as an example, grain boundary[1]) fracture energy is significantly less than the cleavage energy of the microtextural constituents (correspondingly, individual grains).

These issues are discussed in detail in Davidge (1979), Lawn (1993), and are beyond the scope of the present work. The microtexture of the materials of this kind in two-dimensional space could be represented by a random Voronoi froth with the dual Delaunay lattice (Krajcinovic and Rinaldi, 2005a,b). A Voronoi polygon represents a grain of ceramic, a concrete aggregate or a granule of clastic rock whereas a bond in the Delaunay lattices is representative of corresponding interface cohesion[2]. Damage evolution, which reflects accumulation of micro-events of degradation, is a stochastic process dependent on the disorder of the microstructure. The lattice is geometrically disordered since the equilibrium link lengths are normally distributed within the range $\alpha_l\overline{\lambda} \leqslant \lambda \leqslant (2-\alpha_l)\overline{\lambda}$ with $\alpha_l = 0.1$ (if $\alpha_l = 1$ all grains are perfect

[1]Grain boundary is the most common example of the weak interface in brittle materials (Lawn, 1993).

[2]There are issues with representation of materials by spring-network models that have been discussed in detail in the past (see, for example, Ashurst and Hoover, 1976; Curtin and Scher, 1990; Jagota and Bennison, 1994). Nonetheless, we believe that these issues are not of crucial importance herein, bearing in mind the motivation of the work and the considered class of materials. In short, the rationale for the latter is that although adequacy of the spring-network model is not so obvious as for, say, granular materials, its application does not represent mere discretization of a continuum but rather reflects the discrete and disordered nature of the materials whose failure is governed by an "ensemble", a web, of weak interfaces. As Jagota and Berrensen (1994) conclude: "This may not be an issue when dealing with the large disorder and when the goal is to study universal scaling relationships..."

hexagons). Damage is introduced in the network by rupturing of the links, which represent interfacial microcrack formation. The links are nonlinear in compression and linear in tension, with random tensile strength and identical stiffness k. If the critical tensile strain ε_{cr} is reached, permanent rupture occurs and the spring turns into a contact element. The tensile stiffness becomes zero and the link cannot any longer carry tensile forces. Broken links remain active in compression if load reversal occurs in the course of deformation to account for crack closure. The values ε_{cr} are randomly sampled from a uniform distribution starting at zero. This lattice model considers interfacial (hereinafter referred to, more narrowly, as intergranular) microcracks only, which is a reasonable approximation for many ceramics (Davidge, 1979; Lawn, 1993). Since the resolution length of the model is equal to the grain facet, the rupture, i.e. the growth of a microcrack from the initial length to the length of the grain boundary facet, is assumed to be instantaneous. The local fluctuations of the energy barriers (quenched within the material) and the local fluctuations of stress are essential features of the problem at hand, since localization is impossible in the absence of disorder (Anderson, 1958).

Quasi-static displacement-controlled uniaxial tensile tests are simulated on different lattice sizes. The molecular dynamics solver based upon the Verlet's algorithm (Allen and Tidesley, 1994; Krajcinovic and Rinaldi, 2005b; Mastilovic and Krajcinovic, 1999) was adopted. Each simulation is carried on incrementally up to the threshold of failure by applying small displacement steps and by computing the equilibrium configuration at each step. The damage process is tracked during the deformation by recording the number of broken bonds n. The macroscopic data scatter of the $\overline{F}$ vs. $\overline{u}$ and n vs. $\overline{u}$ curves (within-size variability) indicates that $\overline{D}(\overline{\varepsilon}, L)$ is a random variable at any given $\overline{\varepsilon}$ in the softening phase (Fig. 2c,d). The average $\overline{F}$ vs. $\overline{u}$ and n vs. $\overline{u}$ curves from the 10 replicates per size $N = \{24, 48, 96, 192\}$ were considered for the scaling in Krajcinovic and Rinaldi (2005a), with N being the number of grains per lattice side. The original dataset is here sensibly expanded to enhance the accuracy, robustness and precision of the regression analysis. Intermediate lattice sizes $N = \{72, 120\}$ are added and more than 10 runs are collected for smaller lattices. The maximum lattice size is also enlarged. Five extra simulations for $N = 288$ are analyzed but such runs are limited to the hardening phase only for the sake of computational feasibility. The simulation data are summarized in Table 1, for a total of more than 200 simulations as opposed to the original 40.

Table 1. Number of runs per lattice size from MD simulations (old Krajcinovic and Rinaldi (2005a) and new)

Size N	24	48	72	96	120	192	288
Replicates	100	34	30	25	20	13	5

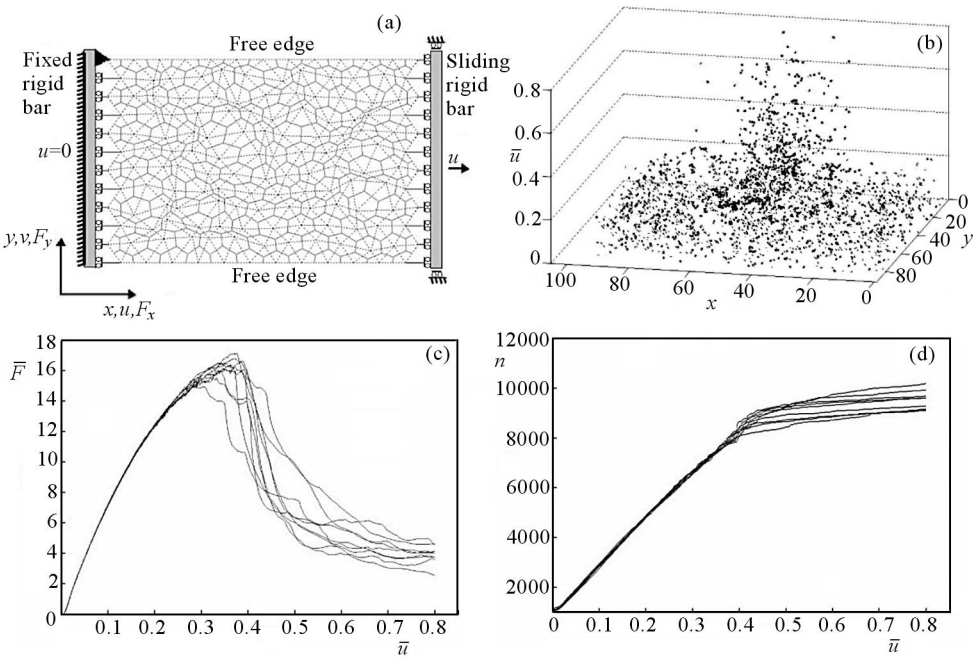

Fig. 2. 12×12 Voronoi/Delaunay graph of the microstructure in tensile test configuration (a); location of broken bonds during a simulation; localization and reduction of damage rate are evident after the transition (b); $\overline{F}$ vs. $\overline{u}$ (c) and n vs. $\overline{u}$ (d) curves for the 10 replicates of $N = 192$

An example of the diffused uncorrelated damage and of the macrocrack from damage localization is displayed in Fig. 3. Only the evolution of such macrocrack can provide the "Crack Growth" defined as "the interval of damage progression from length below which there is negligible POD to an allowable size determined by residual strength requirements" (Goranson, 1993).

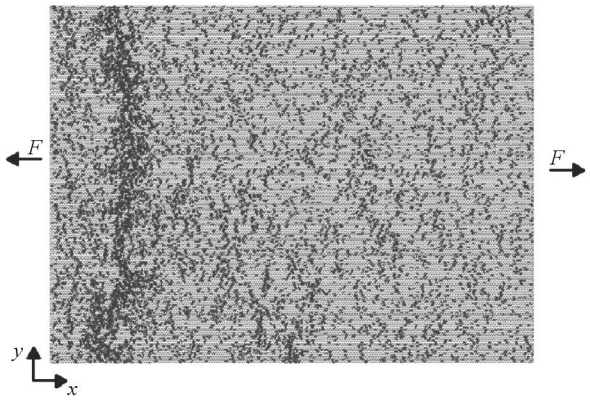

Fig. 3. Damage distribution with macrocrack at the threshold of failure for $N = 192$

3. Statistical (damage) mechanics

The limits of traditional continuum models of damage are discussed at length in literature, e.g. in Krajcinovic and Rinaldi (2005b). Models based upon Eshelby's solution (Mura, 1982), representative volume element (Beran, 1968; Kestin, 1992; Nemat-Nasser and Hori, 1993) and fabric tensor (Krajcinovic, 1996), are suitable only as long as the microstructure is statistically homogenous. Only in this case, the expectation value of damage parameter $\overline{D}$ (the bar above the symbol indicates a macroscopic quantity) is equal to the volume average $\langle D \rangle$ of individual microcracks. Materials are homogeneous when microcracks nucleate in absence of cooperative phenomena, and heterogeneous when clusters of microcracks form. The *threshold of fracture* is reached when one cluster reaches a correlation length equal to the lattice (specimen) size.

Our simulation data indicate that the scaling techniques apply to damage mechanics (Krajcinovic and Rinaldi, 2005a). This statistical model of the disordered microstructure provides analytical expressions of damage parameter. During the hardening phase, i.e. the part of the equation $\overline{\sigma} = \overline{E}^o[1 - \overline{D}(L)]\overline{\varepsilon}$ corresponding to $\partial\overline{\sigma} \geqslant 0$, a simple analytical formula for the damage parameter was obtained from the scaled data

$$\overline{D}(\overline{\varepsilon}, L) = a\overline{\varepsilon} + b\frac{\overline{\varepsilon}^2}{L^\alpha} \tag{3.1}$$

The values $\{\alpha, a, b\} = \{-0.035, 275, -14862\}$ were deduced from simulation data. Instead, the analytical model for the damage parameter during the

softening phase, i.e. the part of the equation $\overline{\sigma} = \overline{E}^o[1-\overline{D}(L)]\overline{\varepsilon}$ corresponding to $\partial\overline{\sigma} \leqslant 0$, was

$$\overline{D} = L^\alpha \overline{D}_p + a_1 L^\alpha \overline{\varepsilon}_s + b_1 L^\alpha L^z \Big[1 - \exp\Big(-\frac{c_1 \overline{\varepsilon}_s}{L^z}\Big)\Big] \tag{3.2}$$

where $\overline{\varepsilon}_s = (\overline{\varepsilon} - \overline{\varepsilon}_{peak})/L^\alpha$, $\overline{D}_p = 0.5$ and $\{a_1, b_1, c_1, z\} = \{15.80, 2.2, 100, -0.52\}$[3] from simulation data (ref. Fig. 7 in Krajcinovic and Rinaldi (2005a)).

4. Damage parameter and constitutive relations

The purpose of this section is the deduction of the analytical constitutive relation

$$\overline{\sigma}(\overline{\varepsilon}, L) = \overline{E}^o[1 - \overline{D}(\overline{\varepsilon}, L)]\overline{\varepsilon} \tag{4.1}$$

from the correct application of the scaling relations (3.1) and (3.2). The damage parameter in the hardening phase was defined in Krajcinovic and Rinaldi (2005a) as

$$\overline{D} = \frac{n(\overline{\varepsilon})}{\mu} L^2 \tag{4.2}$$

where $n(\overline{\varepsilon})$ is the number of broken bonds and μ is a constant deduced from simulations.

4.1. Damage parameter for hardening: rationale

Definition (4.1) is inspired by three observations. First, the strict similarity between the Parallel Bar System (PBS) and the lattice during damage nucleation (Krajcinovic, 1996; Krajcinovic and Rinaldi, 2005b) suggested the following form of damage parameter

$$\overline{D} = \frac{n}{2N_p} \tag{4.3}$$

where N_p is the number of broken links at the peak.

Second, the *log-log* plot of the *average* N_p vs. L in Fig. 3b obtained from simulations demonstrates that N_p for the lattice is a fractal following the power law

$$N_p(L) \cong n(\overline{\varepsilon}_p, L) = \mathrm{e}^{-1.3} L * 1.94 \tag{4.4}$$

[3] As noted in Krajcinovic and Rinaldi (2005a), only one of parameters a_1, b_1, and c_1 is independent.

The fractal exponent is 1.94 with 95% confidence interval $[1.92, 1.96]$. From Eqs. (4.2)-(4.4) the value $\mu = 2\mathrm{e}^{-1.3}$ is estimated, where -1.3 is the (rounded) intercept of the regression line in Fig. 4b. Such value of μ differs from the one reported in (Krajcinovic and Rinaldi, 2005a), previously set to $\mu = 2\mathrm{e}^{-1.6}$. This discrepancy is due to the different datasets used for the statistical analysis. Analogously, the previous estimate of the fractal exponent was 1.96. Since the "expanded" dataset is used here for the regression, the new estimates should be more reliable and accurate. In this respect, the mean square error and the confidence intervals on the regression coefficients (slope and intercept) are tighter. Nevertheless, most of our treatment will refer to the original dataset only and, hence, we will retain the old value $\mu = 2\mathrm{e}^{-1.6}$ in order to legitimately use Eqs.(3.1) and (3.2).

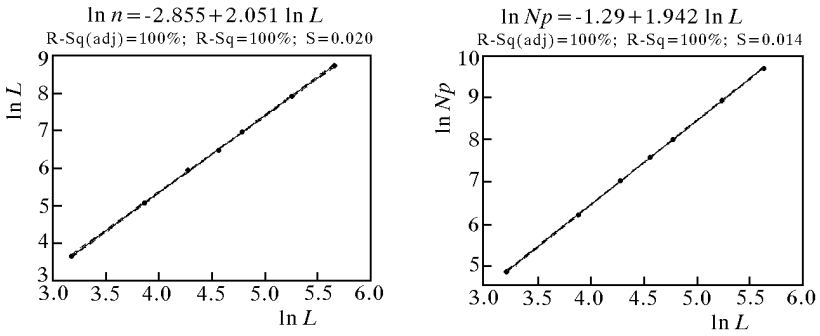

Fig. 4. Fractal behavior of $n(\overline{\varepsilon}, L)$ in the middle of hardening phase (exponent = 2) and at the peak (exponent = 1.94). 95% confidence intervals (dashed line) are very tight

Finally, we replace $L^{1.94}$ with L^2 in Eq. (4.2) because n is a fat fractal with exponent 2 throughout the hardening phase before the transition/peak, as demonstrated by the n vs. L plot in Fig. 4a (taken at an arbitrary $\overline{\varepsilon}$ away from the peak). Furthermore, the n vs. $\overline{\varepsilon}$ curves of different lattice sizes collapsed into a single curve $\overline{D}$ vs. $\overline{\varepsilon}$ during damage nucleation only for the exponent 2 (Fig. 4b in Krajcinovic and Rinaldi, 2005a). This fact, that the relevant damage parameter in the hardening phase is proportional to the density of broken bonds, was already recognized by Hansen *et al.* (1989).

The coefficients of determination R^2 and R^2_{adj} reported by the statistical software MINITAB 14© are rounded to 100% in both graphs in Fig. 4, which proves the high significance/quality of the regression analysis ($R^2 = 1$ indicates perfect linear correlation ([17]; Montgomery *et al.*, 2001)). The regression on the seven sizes $N = \{24, 48, 72, 96, 120, 192, 288\}$ provides a 2-decimal digits precision for the fractal exponents, which is satisfactory. The size range spans over one order of magnitude.

4.2. Damage parameter for softening

With $\overline{D}$ defined as in (4.2), the $\overline{D} - \overline{\varepsilon}$ curves were scaled in Krajcinovic and Rinaldi (2005a) to obtain Eqs. (3.1) and (3.2). While Eq. (3.1) is a suitable definition of damage parameter for the hardening phase, Eq. (3.2) is not a valid damage parameter for the softening phase. The lattice is a spring-network and the corresponding secant stiffness $\overline{E}(L) = \overline{E}^o[1 - \overline{D}(\overline{\varepsilon}, L)]$ is positive-definite (Krajcinovic, 1996). Hence, the "proper damage parameter" must always be $0 \leqslant \overline{D} \leqslant 1$ and should monotonically approach $\overline{D} = 1$ at failure ($\overline{E}_{failure} = 0$), either discontinuously or continuously depending on whether the failure transition is of the first order or second order. These two constraints were not accounted for in the scaling of the softening data. Therefore, while expression (3.1) is perfectly legitimate, definition (3.2) is still incomplete.

The number of broken links $n(\overline{\varepsilon})$ is an indicator of the total damage. The parameter $\overline{D}$ supplies just the normalization, like in Eq. (4.3), and possibly renders this information scale invariant. One fundamental idea in our framework is that hardening and softening phases are independent sequential processes. The microcracks nucleation is driven by a fat fractal with fractal exponent 2 for the most part and by a proper fractal with exponent 1.94 at the peak of stress-strain response. Such driving set changes at the transition, i.e. an appropriate denominator (normalization number) should replace μL^2 in (4.2). The following form of damage parameter is assumed in the softening phase

$$\overline{D}(\overline{\varepsilon}, L, n) = \frac{n(\overline{\varepsilon}_{peak}, L)}{\mu L^2} + \frac{\Delta n(\overline{\varepsilon}, L)}{X(L)} \tag{4.5}$$

where $\Delta n = n(\overline{\varepsilon}, L) - n(\overline{\varepsilon}_{peak}, L)$ is the number of broken bonds in the softening phase. The analytical expression for Δn follows from (3.2) and (4.2) as

$$\Delta n(\varepsilon, L) = \mu L^2(\overline{D} - L^{\alpha}\overline{D}_p) = \mu L^2\Big\{a_1 L^{\alpha}\overline{\varepsilon}_s + b_1 L^{\alpha} L^z\Big[1 - \exp\Big(-\frac{c_1\overline{\varepsilon}_s}{L^z}\Big)\Big]\Big\} \tag{4.6}$$

which is essentially the information conveyed by Eq. (3.2). Eq.(4.6) is equivalent to magnifying the scaled data in the softening phase by a factor μL^2. The constitutive relations for the hardening and softening phases can be rewritten as

$$\overline{\sigma} = \begin{cases} \overline{E}^o\Big[1 - \dfrac{n(\overline{\varepsilon}, L)}{\mu L^2}\Big]\overline{\varepsilon} & \text{for} \quad \overline{\varepsilon} \leqslant \overline{\varepsilon}_{peak} \\ \overline{E}^o\Big[\Big(1 - \dfrac{N_p}{\mu L^2}\Big) - \dfrac{\Delta n(\overline{\varepsilon}, L)}{X(L)}\Big]\overline{\varepsilon} & \text{for} \quad \overline{\varepsilon} > \overline{\varepsilon}_{peak} \end{cases} \tag{4.7}$$

Then, $X(L)$ in the denominator of (4.5) and $(4.7)_2$ is what needs to be defined. The 3D plot of microcracks location vs. simulation time in Fig. 2b highlights

the contrast between the uncorrelated and uniformly distributed damage nucleation and the highly correlated and localized damage propagation. From this viewpoint, a fractal exponent close to one makes intuitive sense for the invariant set driving the propagation, as much as a fat fractal suits the phenomenology of the nucleation.

A deductive reasoning based upon statistical methods is used to reach the data driven choice for $X(L)$. By assuming that $(4.7)_2$ is the right form of the model, one can write

$$\widehat{\overline{\sigma}}_i(\overline{\varepsilon}_i, \Delta n_i, \beta) = \overline{E}^o\Big[\Big(1 - \frac{N_p}{\mu L^2}\Big) - \beta \Delta n_i\Big]\overline{\varepsilon}_i \tag{4.8}$$

where $\beta(L) = 1/X(L)$, Q is the number of numerical observations used for the regression and $\widehat{\overline{\sigma}}_i$ is the estimate of stress value at $\overline{\varepsilon}_i$ and Δn_i from the model for $i = 1, 2, \ldots, Q$. Since the model is linear in the unknown parameter β, the "ordinary least squares" method can be used to compute a minimum unbiased estimator $\widehat{\beta}$ of β (Montgomery *et al.*, 2001). The mean square error function for this model is

$$\mathrm{Err}(L) = \sum_{i=1}^{Q} (\overline{\sigma}_i - \widehat{\sigma}_i)^2 = \sum_{i=1}^{Q} \Big(\overline{\sigma}_i - \overline{E}^o\Big[\Big(1 - \frac{N_p}{\mu L^2}\Big) - \widehat{\beta}\Delta n_i\Big]\overline{\varepsilon}_i\Big)^2 \tag{4.9}$$

which is the sum of the squared deviations between the simulation data and the predicted value over Q. The error function is minimized with respect to $\widehat{\beta}$ by setting $\partial \mathrm{Err}/\partial\widehat{\beta} = 0$. The calculations lead to

$$\widehat{\beta}(L) = \frac{\sum_{i=1}^{Q}\Big[\Big(1 - \frac{N_p}{\mu L^2}\Big)\overline{E}^o\overline{\varepsilon}_i - \overline{\sigma}_i\Big]\Delta n_i \overline{\varepsilon}_i}{\sum_{i=1}^{Q} \overline{E}^o \overline{\varepsilon}_i^2 \Delta n_i^2} \tag{4.10}$$

which depends on the lattice size L. Finally, the formula for the estimate $\widehat{X}(L)$ is

$$\widehat{X}(L) = \widehat{\beta}^{-1}(L) = \frac{\sum_{i=1}^{Q} \overline{E}^o \overline{\varepsilon}_i^2 \Delta n_i^2}{\sum_{i=1}^{Q}\Big[\Big(1 - \frac{N_p}{\mu L^2}\Big)\overline{E}^o\overline{\varepsilon}_i - \overline{\sigma}_i\Big]\Delta n_i \overline{\varepsilon}_i} \tag{4.11}$$

The results of Eq. (4.11) are marked in Fig. 5 by circles for the sizes $N = \{24, 48, 72, 96, 120, 192\}$. The linear fit through the six $\widehat{X}(L)$ values matches the results very well, as indicated by a coefficient of determination close to unity ($R^2 = 0.9971$; $R^2_{adj} = 0.997$). The equation of the regression line is

$$X(L) = \mu_2 L + \mu_3 = 65.07L - 1038 \tag{4.12}$$

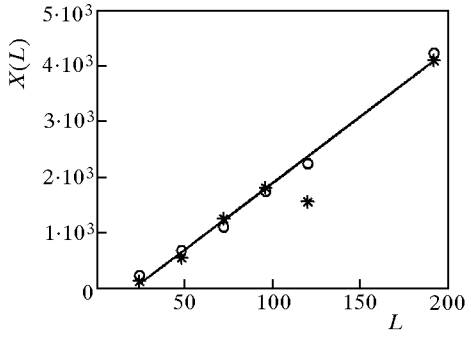

Fig. 5. Comparison of $X(L)$ estimates from (4.11) for the 6 average Δn (circles) and for 6 random replicates per each size $N = \{24, 48, 72, 96, 120, 192\}$ (asterisks)

with 95% confidence intervals $(60.38, 69.76)$ and $(-1589, -585.6)$ for the slope and the intercept respectively. This linear model supplies $X(L)$ in Eqs. (4.5) and $(4.7)_2$.

Such a result seems to confirm the above supposition from phenomenology about the linear dependence of X on L. Nevertheless, more data points are required to increase the precision and tighten the relatively wide confidence intervals. For very large lattices, when the intercept becomes negligible $(1038 \ll 65.07L)$, the relations (4.5) and $(4.7)_2$ are nicely approximated for $\overline{\varepsilon} > \overline{\varepsilon}_{peak}$ by

$$\begin{aligned} \overline{\sigma} &= \overline{E}^o \Big[\Big(1 - \frac{N_p}{\mu L^2} \Big) - \frac{\Delta n(\overline{\varepsilon}, L)}{65L} \Big] \overline{\varepsilon} \\ \overline{D}(\overline{\varepsilon}, L, n) &= \frac{n(\overline{\varepsilon}_{peak}, L)}{\mu L^2} + \frac{\Delta n(\overline{\varepsilon}, L)}{\mu_2 L} = \frac{N_p}{\mu L^2} + \frac{\Delta n(\overline{\varepsilon}, L)}{65L} \end{aligned} \tag{4.13}$$

Relation $(4.13)_2$ implies a discontinuity in the derivative of the damage parameter $\overline{D}(\overline{\varepsilon}, L, n)$ due to the abrupt change of the denominator from L^2 to L at the hardening-softening transition. While $n(\overline{\varepsilon})$ is a C^1 continuous function at $\overline{\varepsilon}_{peak}$, the damage is C^0 continuous and the damage rate $\partial n(\overline{\varepsilon})/\partial \overline{\varepsilon}$ discontinuous, in agreement with Fig. 2b and Fig. 2d.

The choice of the Q data points to be used in the evaluation of (4.11) is crucial for the accuracy of $\widehat{X}(L)$ and depends on what part of the response is of interest. This analysis aimed at capturing the steepest descent of the softening regime after the transition and only the corresponding points (about 25% of softening dataset) were selected to minimize the model error in that part. The performance of the analytical expressions (4.7) are compared in Fig. 6a and

Fig. 6b against the original average simulation data for $N = 48$ and $N = 96$, respectively.

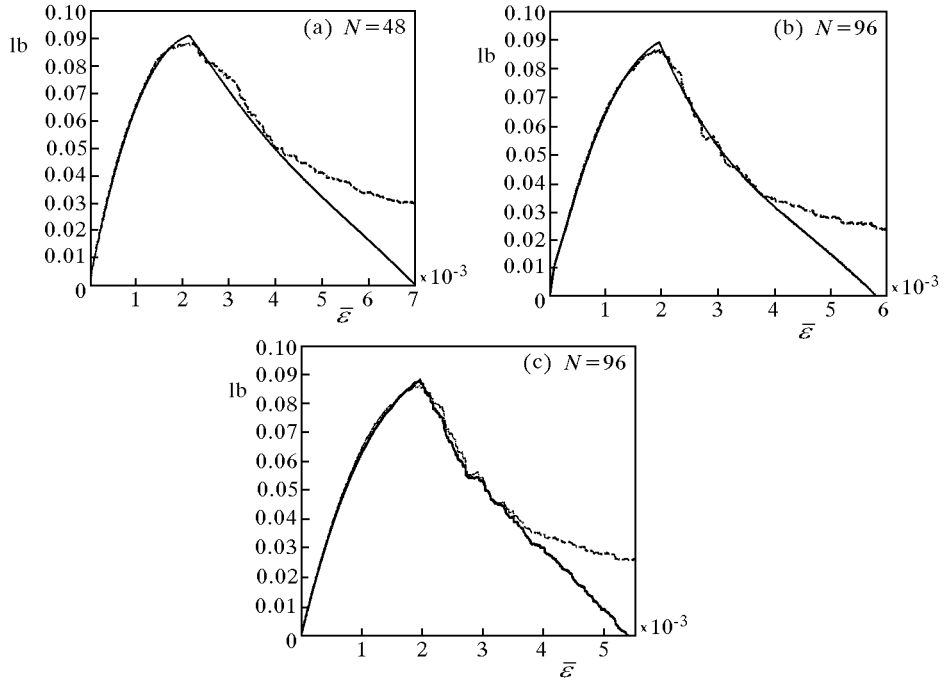

Fig. 6. Overall model fitting for $N = 48$ and $N = 96$ with X from OLS, Eq. (4.11); $n(\overline{\varepsilon}, L)$ and $\Delta n(\overline{\varepsilon}, L)$ are estimated via scaling relations. (c) Improved fit for $N = 96$ when numerical data are used directly for $n(\overline{\varepsilon}, L)$ and $\Delta n(\overline{\varepsilon}, L)$ instead of scaling relations in the constitutive relations (4.7)

4.3. Interpretation and limits of relations for softening

The model closely estimates the numerical data for most of the design space. Concerns might arise about the accuracy of relations (4.5) and $(4.7)_2$ for the softening phase. The performances of the model are determined essentially by two aspects:

1. The selected model form (4.5) for the damage parameter $\overline{D}$
2. The accuracy of the estimates $n(\varepsilon, L)$ and $\Delta n(\varepsilon, L)$ from scaling.

At first, by assuming that the model form (4.5) is correct, we focus on the second issue. The scaling relations for $n(\varepsilon, L)$ and $\Delta n(\varepsilon, L)$ from Eqs. (3.1) and (4.6) refer to the average data, obtained by first averaging the original

$n - \overline{\varepsilon}$ curves of individual replicates for each size and then, after scaling, by fitting a regression model to the scaled data. This twofold "filtering" process smeared out the irregularities characteristic of each replicate (compare Fig. 2d with Fig. 7 in Krajcinovic and Rinaldi (2005a). Thus, while on one side we obtain smooth analytical relations capable of estimating the average microcracks number for any lattice size, on the other side the characteristic "details" of each individual replicate are lost. Fig. 6c shows the model obtained from Eqs. (4.6) for $N = 96$ when average n and Δn from simulations are used in place of the scaling relations. The new estimates "shadow" the simulation data of the softening phase better than before. Evidently a better knowledge of n and Δn leads to a more accurate constitutive model. For these simulations, the difference between the estimates of n and Δn from scaling relations and from simulations, never exceeded 10% for any lattice size. However, the predictive power does not change significantly.

To assess the other issue about the appropriateness of the selected model form, Eqs. (4.5) and (4.7) are tested against individual lattice simulations. Six individual replicates for $N = \{24, 48, 96, 72, 120, 192\}$ are randomly picked. This time the values of n, Δn and N_p are obtained directly from the simulation. As the model is satisfactory for the hardening phase, the previous estimate of μ is kept for all cases. Instead, the parameter $X(L)$ in (4.5) is re-estimated for each replicate via Eq. (4.11). These new values of $\widehat{X}(L)$ are marked in Fig. 5 by asterisks and fall reasonably close to the line (4.12) for the average values. The corresponding six constitutive models are shown in Fig. 7. The agreement between models (full line) and numerical data (dotted) is remarkable. Complex patterns and discontinuities are well-captured for most of the softening phase. The models are in general able to reproduce the response also after the change of curvature following the initial steep descendent from the peak. These results are achieved by re-estimating merely the sole parameter $X(L)$. The conclusions are the following:

- The choice of the model form in Eq. (4.5) seems appropriate
- A simple model can reproduce a variety of softening responses
- The greatest accuracy is achieved by calibrating the constitutive relations on an individual simulation; the same constitutive relations of the mean response can be used by simply re-estimating $X(L)$ from the simulation data
- A greater accuracy for the individual replicate is determined by the usage of un-filtered simulation data for n and Δn in place of the average estimates.

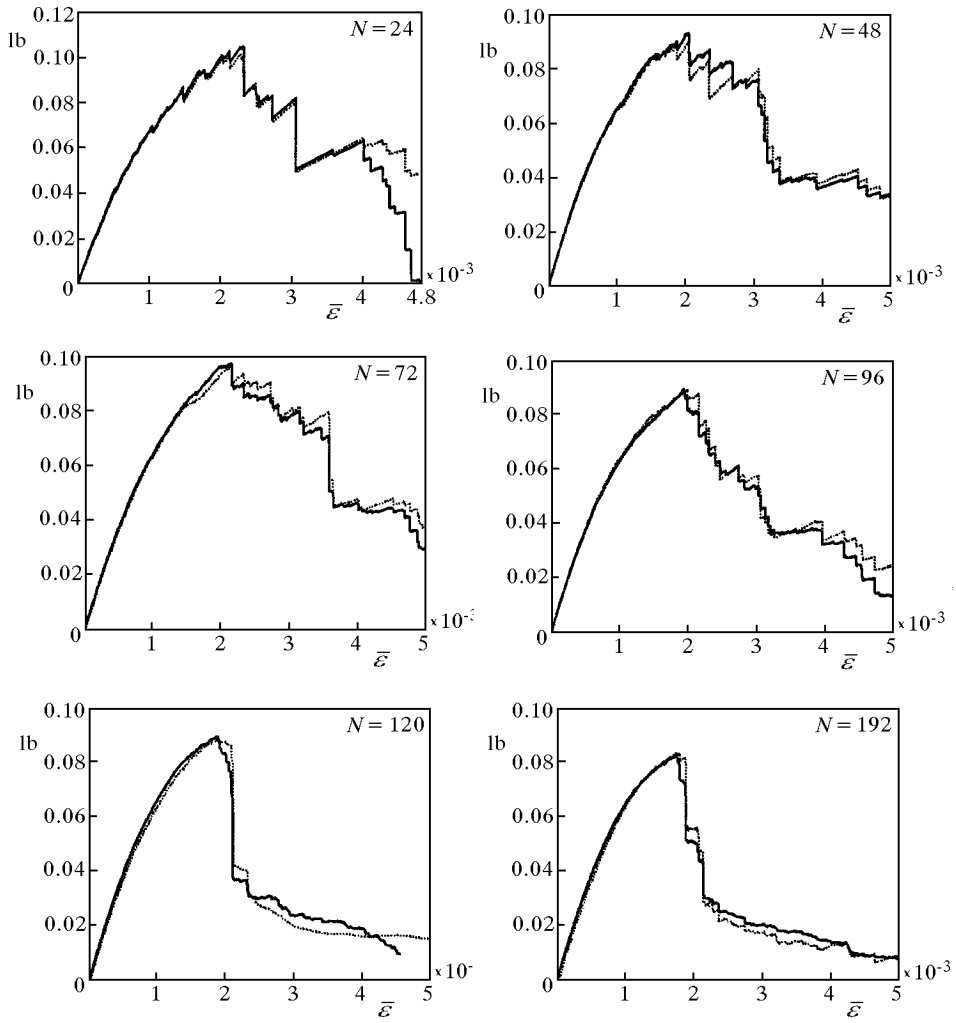

Fig. 7. Responses of customized model (4.5) and $(4.7)_2$ (full line) vs. simulation data (dotted line) for six individual random replicates for $N = \{24, 48, 72, 96, 120, 192\}$

The findings corroborate and clarify the proposed constitutive model. The last conclusion pointed out that the continuous approximation of $n(\bar{\varepsilon}, L)$ and $\Delta n(\Delta\bar{\varepsilon}, L)$ from scaling relations overlooks large discontinuities in the $n - \bar{\varepsilon}$ data registered in connection with large avalanches, both at the onset of damage localization and afterwards. The lattice response of the softening phase has a saw-toothed appearance on the macro-scale due to large avalanches, whose signatures are sudden vertical drops in the stress level alternated to linear ela-

stic "climbs". Such vertical drops observable for each replicate (Fig. 7) totally disappear in the average curves in Fig. ??a, leaving space to a "fictitious" more gentle descendent. An accurate model matching the data from an individual test is achievable when the specific details of $\Delta n(\Delta\overline{\varepsilon}, L)$ are accounted for on a case-by-case basis. Conversely, the scaling relations (3.1) and (3.2) represent an average behavior and offer the general "trend" for all lattice sizes. The results outline the potential of a statistical damage mechanics model, which go well beyond the limits of traditional continuum approach.

5. Conclusion and summary

The statistical mechanics theory and the application of the theory have been presented in the previous paper (Krajcinovic and Rinaldi, 2005a). This paper is committed to constitutive modeling, failure and damage tolerance. The results offered in this paper display the effectiveness of the statistical damage model in the study of the softening regime and failure. The numerical data produced with this approach could not be generated by classical continuum damage mechanics.

The scale-invariant damage curves proposed in Krajcinovic and Rinaldi (2005a) are re-examined and finalized herein to obtain the analytical constitutive relations (4.7) for the entire damage process. The damage parameter is properly defined not only in the hardening phase but also in the softening phase to attain this result. In the hardening phase the process is driven by a fractal set of exponent two, while in the softening phase the fractal dimension tends towards one. Additional numerical data improved the precision of the statistical analysis. The present paper not only reorganizes and reinforces some of the ideas originated in the inspiring work of Hansen *et al.* (1989), but also addresses successfully some of the open questions by adopting a rather different methodology. This study outlines the importance of the statistical methods, such as ordinary least squares, maximum likelihood and hypothesis testing, for the selection of the model parameters. These techniques are the basis for data-driven reasoning and decision making in damage tolerance.

Acknowledgments

This research is sponsored by the Mathematical, Information and Computational Science Division, Office of Advanced Scientific Computing Research, U.S. Department of Energy under contract number DE-AC05-00OR22725 with UT-Battelle, LLC. The support of the Ministry of Science and Environmental Protection of Republic of Serbia

(under contract numbers 1793 and 1865) to S. Mastilovic is gratefully acknowledged. The authors address a special thank to Dr S. Simunovic at ORNL and prof. Y.C. Lai at ASU for valuable support.

References

1. ALLEN M.P., TILDESLEY D.J., 1994, *Computer Simulation of Liquids*, Clarendon Press, Oxford, UK
2. ANDERSON P.W., 1958, Absence of diffusion in certain random lattices, *Phys. Rev.*, **109**, 1492-1505
3. ASHURST W.T., HOOVER W.G., 1976, Microscopic fracture studies in the two-dimensional triangular lattice, *Phys. Rev. B*, **14**, 4, 1465-1473
4. BERAN M., 1968, *Statistical Continuum Theories*, Wiley, New York
5. CURTIN W.A., SCHER H., 1990, Brittle fracture in disordered materials, *J. Mater. Res.*, **5**, 3, 535-553
6. DAVIDGE R.W., 1979, *Mechanical Behavior of Ceramics*, Cambridge Univ. Press, Cambridge, UK
7. GORANSON U.G., 1993, Damage tolerance – facts and fiction, *14th Plantema Memorial Lecture Presented at the 17th Symposium of the International on Aeronautical Fatigue*, Stockholm, Sweden
8. HANSEN A., ROUX S., HERRMANN H.J., 1989, Rupture of central-force lattices, *Phys. Fracture*, **50**, 517-522
9. JAGOTA A., BENNISON S.J., 1994, Spring-network and finite element models for elasticity and fracture, *Proceedings of a Workshop on Breakdown and Nonlinearity in Soft Condensed Matter*, K.K. Bardhan, B.K. Chakrabarti, A. Hansen (edit.), Springer-Verlag Lecture Notes in Physics, Berlin, Heidelberg, New York
10. KACHANOV L.M., 1958, On the time to failure under creep conditions, *Izv. AN SSSR, Ot. Tekhn. Nauk*, **8**, 26-31
11. KESTIN L., 1992, Local-equilibrium formalism applied to mechanics of solids, *Int. J. Solids Structures*, **29**, 14/15, 1827-1836
12. KRAJCINOVIC D., 1996, *Damage Mechanics*, North-Holland Series in Applied Mathematics and Mechanics, Vol. 41, Elsevier, Amsterdam
13. KRAJCINOVIC D., BASISTA M., 1991, Rupture of central-force lattices revisited, *J. de Physique I*, **1**, 241-225

14. KRAJCINOVIC D., RINALDI A., 2005a, Statistical damage mechanics – 1. Theory, *J. of Applied Mechanics*, **72**, 76-85

15. KRAJCINOVIC D., RINALDI A., 2005b, Thermodynamics and statistical physics of damage processes in quasi-ductile solids, *Mech. Mater.*, **37**, 299-315

16. LAWN B., 1993, *Fracture of Brittle Solids*, Cambridge Univ. Press, Cambridge, UK

17. MINITAB 14©, on-line manual

18. MASTILOVIC S., KRAJCINOVIC D., 1999, Statistical models of brittle deformation. Part II: Computer simulations, *Int. J. Plasticity*, **15**, 427-456

19. MONTGOMERY D.C., PECK E.A., VINING G.G., 2001, *Introduction to Linear Regression Analysis*, Wiley

20. MURA T., 1982, *Micromechanics of Defects in Solids*, Martinus Nijhoff Publishers, The Hague

21. NEMAT-NASSER S., HORI M., 1993, *Micromechanics: Overall Properties of Heterogeneous Materials*, North-Holland Series in Applied Mathematics and Mechanics, Vol. 37, Elsevier, Amsterdam

Statystyczna mechanika uszkodzenia - związki konstytutywne

Streszczenie

Statystyczny model uszkodzenia, przedstawiony przez autorów w innej pracy, zastosowano tu do sformułowania analitycznych związków konstytutywnych w zakresie wzmocnienia i osłabienia dla dwuwymiarowych modeli sieciowych. Wprowadzono odpowiednią definicję parametru uszkodzenia w zakresie osłabienia. Uzyskane wyniki potwierdzają, że wprowadzony model analityczny można stosować do badania osłabienia i zniszczenia materiałów. Praca stanowić może podstawę do ustalenia norm technicznych uszkodzenia stosowanych w przemyśle lotniczym

Manuscript received October 24, 2005; accepted for print March 27, 2006